

# Characterization of a spark-based Long Period Grating (LPG) recording system

Frederico Campos Freitas<sup>1</sup>, Fabiano Kuller<sup>2</sup>, Márcia Muller<sup>2</sup>, José Luís Fabris<sup>2</sup>, Cyro Ketzer Saul<sup>1,\*</sup>

<sup>1</sup> Departamento de Física – Universidade Federal do Paraná (UFPR)

Centro Politécnico – Jd. das Américas – 81531-990 – Curitiba – PR – Brasil

<sup>2</sup> Departamento de Física - Universidade Tecnológica Federal do Paraná (UTFPR)

Av. Sete de Setembro, 3165 – 80230-901 – Curitiba – PR - Brasil

\*Corresponding author: 55 (41) 33613404 - cyro@fisica.ufpr.br

## Abstract

Developed in the 90's, the Long Period Grating (LPG) consists of a periodic refractive index modulation over a specific length of a single mode optical fiber used in telecommunications. The created index grating promotes coupling between the core and cladding modes, resulting in a transmitted spectrum that shows some attenuation dips over a well-defined range of wavelengths. Any change in the effective refractive indexes of the fiber due to changes in the surrounding environment refractive index, stress or temperature generates a shift in the LPG resonance wavelength. Based on this effect it is possible to fabricate both physical and chemical sensors. This work presents the preliminary characterizations of LPGs fabricated using a locally developed thermal spark-based recording equipment, which allows point recording over a 5.5 cm range, over the fiber length. The recording system is controlled by a LabView 6.1 developed software, through the parallel port of a personal computer (PC). The software allows controlling the length and period of the recorded gratings, with a 1.25 μm resolution, as well as the electrical arc duration used in the recording process.

**Keywords:** Long period gratings, LPG, sensors, fabrication process

## Introduction

Long period gratings (LPGs) as well as fiber Bragg gratings (FBGs) are optical fiber based devices that can be used as sensors. Developed in the nineties they consist of a periodic modulation in the refractive index produced over a standard communication optical fiber. The difference between then relays on the period of grating, which for the FBG is about the order of magnitude of the transmitted light wavelength. For LPGs the grating period is about two orders of magnitude bigger than the light wavelength (200 to 700 μm) [1]. While for FBG the recorded grating promotes the coupling between the core co-propagating and contra-propagating modes, for LPG this coupling occur between core and cladding propagation modes. In both cases the coupling leads to one or more attenuation bands in the transmitted spectra of the fiber. In the case of FBGs the band can be detected in both transmission and reflection configuration. For transmission the band appears as a dip in the spectrum and for reflection as a peak. For LPGs it is only possible to detect the transmitted spectrum, which presents only attenuation dips. Since the coupling between the core and cladding modes is

highly sensitive to the external medium refractive index, mechanical stress or temperature subjected to the fiber such sensors can be used as physical or chemical sensors. For LPGs the attenuation dip position in the transmitted spectrum is calculated using

$$\lambda_{abs} = \Lambda (n_{core}(\lambda) - n_{clad}^i(\lambda)) \quad (1)$$

where  $n_{core}(\lambda)$  is the effective refractive index of the core mode,  $n_{clad}^i(\lambda)$  is the effective refractive index of the  $i^{th}$  cladding mode and  $\Lambda$  is the period of recorded grating. For FBGs both attenuation dip position, in the transmitted spectrum, and peak position, in the reflected spectrum, are determined by

$$\lambda_B = 2 \cdot n_{eff} \cdot \Lambda \quad (2)$$

where  $\lambda_B$  is the Bragg wavelength,  $n_{eff}$  is the effective refractive index of the fiber core mode and  $\Lambda$  is the grating period. The versatility of those sensors, associated to its low cost and possibility of integration to built networks of multiple sensors is being drawing a great deal of attention towards applications development. Other important factor is associated to the working principle of those sensors. The optical fiber is immune to all kinds of

electromagnetic interferences and the sensors are harmless to explosive environments.

Regarding the recording process, FGBs are usually produced using UV radiation over photosensitive fibers due to the small recording periods ( $\Lambda$ ), in the range of micrometers [2]. As well as FGBs, the LPGs can be recorded using UV radiation, but since the recording periods ( $\Lambda$ ) are a few orders of magnitude bigger, other thermal processes can be used, as CO<sub>2</sub> laser pulses [3] or electrical arc discharges [4] [5] [1]. In the specific case of electrical arc discharges the low cost of the equipment becomes an attractive. In this work we present the characterization of the first LPGs recorded with electrical arc discharge equipment fully developed in our laboratory.

## Experimental

### The recording equipment

Since most arc discharge-recording systems in the literature use standard fusion-splicing machines [4][5], based on the system simplicity and low cost, we decided to construct a complete recording system with full parameter control. The equipment we have developed consists of four parts: the spark gap; the positioner; the high voltage power source; and the computer interface. The spark gap uses two Tungsten TIG welding electrodes about 1 mm apart, mounted on the positioner. The positioner is an Aerotech x-translator driven by a step motor. The high voltage power consists of a high voltage neon lamp transformer, fully rectified, that generates the electric discharge on the spark gap. The computer interface has a set of eight discrete Darlington transistors connected to the parallel port of a personal computer (PC). It also includes one digital input to pick-up the zero of the positioner.

The working principle of our system is based on the thermal and mechanical stresses generated over the optical fiber to create the periodic refractive index change. The fiber is placed vertically in such way that it passes between the two electrodes and it stays still over the entire recording process. The bottom extremity of the fiber is attached to a small weight, to produce mechanical stress. After the recording is started the positioner is moved backwards to zero position, and then moved forward to the first recording position. This procedure eliminates backlash position errors. When it stops the high voltage discharge is turned on. The system allows controlling both discharge power and time length. The heat generated is enough to soften the optical fiber locally allowing the tapering of the fiber. In some cases the deformation can be visualized with optical microscopy, as shown in figure 1. To continue the process the positioner is moved to the

next recording place, repeating the process until all the points are recorded. We have a 5.5 cm available recording range. Most parameters of the recording process are set previously in the PC using a LabView 6.1 developed software interface.

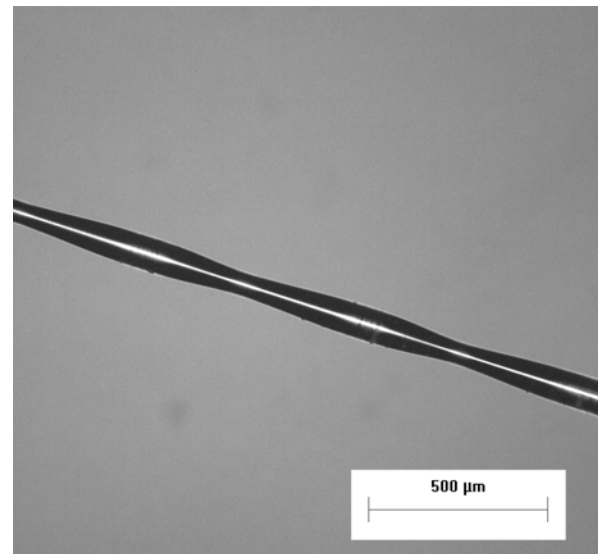


Figure 1. Physical deformation of the fiber due to thermal effects combined with mechanical stress.

### LPG Samples

The LPG samples were recorded on standard Corning SMF-28 single mode optical fibers suited to operate in the *O* (1260 to 1360 nm), in the *C* (1530 to 1565 nm) and in the *L* (1565 to 1625 nm) bands. The plastic cladding of the fibers was removed in the recording region using chloroform. The mechanical stress was generated using a 4.32 g weight attached to the lower end of the fiber, and the electrical arc was applied to the fiber during 1s. The power of the arc, measured in the primary of the high voltage transformer was 27.8 W. Table 1 shows the period and the number of recorded points for each sample.

Table 1. Sample recording parameters.

Sample Number	Grating Period $\Lambda$ ( $\mu\text{m}$ )	Number of Points
136	400	40
138	500	40
139	500	80

After recording, the fibers were visually inspected to check the visibility of the recorded points. The gratings were visible for all recorded samples. The fiber characterizations were performed using a LED source (Luminent MREDSP5003, central wavelength at 1530.3 nm and half bandwidth of 52.0 nm) and an Optical Spectrum Analyzer (OSA) Anritsu MS9710B (0.1 nm resolution, wavelength stability of  $\pm 5$  pm and wavelength accuracy of  $\pm 0.05$  nm). Each sample was measured as recorded

in air, dipped in pure water and in pure ethanol, keeping constant the temperature and applied strain.

**Results and Discussion**

Figure 2 shows the obtained spectra with sample 136 that has 400µm of nominal period ( $\Lambda$ ) with 40 recorded points. By means of an inspection of the image obtained with the optical microscope (figure 1), the real grating period was estimated to be 638 µm. This may be easily understood if we consider the fact that the length of the fiber increases during the recording process due to softening. Even though the nominal grating period was 400 µm, the effective period obtained was bigger.

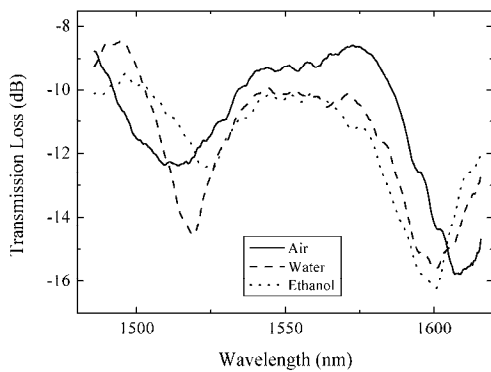


Figure 2. Transmission loss spectra for sample 136 ( 40 points and 400 µm period ) in air, dipped in pure water and in pure ethanol.

In this figure we also notice the shifts of the peaks when the recorded region is dipped in water and ethanol. It is interesting to notice that the dip at 1513 nm presented a displacement toward higher wavelengths while the dip at 1610 nm presented a displacement toward lower wavelengths.

Figure 3 shows the spectra obtained with sample 138 that presents 40 recorded points with a nominal period of 500 µm.

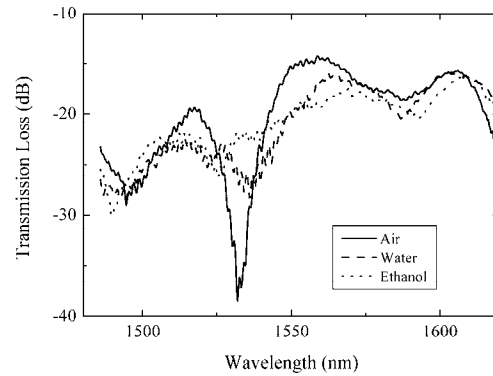


Figure 3. Transmission loss spectra for sample 138 ( 40 points and 500 µm period ) in air, dipped in pure water and in pure ethanol.

Since the dips move toward higher wavelengths as the recording period ( $\Lambda$ ) increases [1] it is possible to suppose that the dip at 1496 nm is not visible for sample 136, and the dip at 1533 nm corresponds to dip at 1513 nm for 136. In this case we notice that the dip at 1496 nm moves toward lower wavelengths under effect of both water and alcohol. It is interesting to notice that the dip at 1533 shifts toward higher wavelengths under effect of water, which is consistent with the effect observed in sample 136, while it moves in the opposite direction under ethanol. This effect is not yet understood but the signal over attenuation under ethanol has to be taken into account and might have masked the dip measurement.

Table 2 presents dip absolute positions and relative shifts for each sample under air, water and ethanol influence. As expected [6] [7], the analysis of the data clearly indicates that ethanol always promotes the strongest shift of the dips for both samples where the dips could be measured. The refractive indexes of the samples measured with an Abbe refractometer were 1.333 (water) and 1.365 (ethanol).

Table 2. Dip absolute positions and displacements using air as reference.

Sample	Dip position			Dip shift (ref. Air)			
	Air	Water	Ethanol	Water		Ethanol	
	Nm	nm	nm	nm	%	nm	%
136	1513	1519	1524	6	0,40%	11	0,73%
	1610	1601	1598	-9	- 0,56%	-12	- 0,75%
138	1496	1492	1490	-4	- 0,27%	-6	- 0,40%
	1533	1536	1525	3	0,20%	-8	- 0,52%

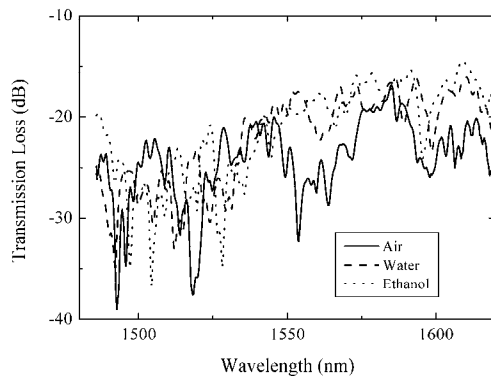


Figure 4. Transmission loss spectra for sample 139 ( 80 points and 500  $\mu\text{m}$  period ) in air, dipped in pure water and in pure ethanol.

Figure 4 shows the spectra obtained for sample 139, that presents 80 recorded points with a nominal period of 500  $\mu\text{m}$  under air, water and ethanol, as the previous ones. In this case the number of recorded points, what is proportional to the coupling strength, was so elevated that almost all the light coupled with the cladding and was lost. The dips are practically undetectable within the noise, even in air.

Our results indicate that our electrical arc recording parameters were too strong, which is also evidenced by the big physical deformations observed in the recorded region. Although *P. Palai et al.* [4] sustains that the physical deformation is not necessary to promote the coupling between core and cladding modes it may be possible that strong deformations in the sensitive region generate intensity losses over the full spectrum range, as observed for sample 139, shown in figure 4.

## Conclusions

We have developed a thermo-mechanical LPG recording system based on electric arc discharges that allows controlling recording period ( $\Lambda$ ), number of recorded points, discharge power and duration. The samples were recorded on standard communication optical fibers changing period and number of points and keeping the other parameters unchanged. Samples were therefore characterized using an OSA exposing the sensitive regions to air, pure water and pure ethanol. Results indicate that the samples are capable of detect refraction index changes in the surrounding environment as

expected for such type of sensors. We were able to identify changes in dip position due to recording period change. We were also able to verify that the effective recorded period is greater than the nominal period due to fiber elongation during the recording process. The elongation was generated by fiber softening and mechanical stress. We observed that both gratings recorded with 40 points the attenuation dips are well defined, while for the grating with 80 points the resulting spectrum is over-attenuated. This might be associated with the excessive tapering observed in the recorded area, increasing the light losses over the full wavelength range. The shift for the peaks, as the refractive index of the surrounding media changed, presented the expected behavior mentioned by *X. Shu et al.* [8].

## References

- [1] G. Rego, O. Okhotnikov, E. Dianov and V. Sulimov, *High-temperature stability of long-period fiber gratings produced using an electric arc*, J. OF LIGHTW TECHN 19 (2001) 1574-1579
- [2] A. Othonos, K. Kalli, *Fiber Bragg Gratings*. Artech House, Inc. (1999)
- [3] C. Narayanan, H.M. Presby, A.M. Vengsarkar, *Band-rejection fibre filter using periodic core deformation* ELECTR LETT 33 (1997) 280-281
- [4] P. Palai, M.N. Satyanarayan, M. Das, K. Thyagarajan, B.P. Pal, *Characterization and simulation of long period gratings fabricated using electric discharge*, OPT COMM 193 (2001) 181-185
- [5] G.M. Rego, J.L. Santos and H.M. Salgado, *Polarization dependent loss of arc-induced long-period fibre gratings*, OPT COMM 262 (2006) 152-156
- [6] R. Falate, R.C. Kamikawachi, J.L. Fabris, M. Müller, H.J. Kalinowski, *Fiber optic hydrocarbon sensors based on long period gratings*. Journal of Microwaves and Optoelectronics, Brasil, v. 3 (2004) 47-55
- [7] R. FALATE, R.C. Kamikawachi, M. Müller, H.J. Kalinowski, J.L. Fabris, *Fiber Optic Sensors for Hydrocarbon Detection*. Sensors and Actuators B-Chemical, 105 (2005) 430-436
- [8] X. Shu, D. Huang, *Highly sensitive chemical sensor based on the measurement of the separation of dual resonant peaks in a 100- $\mu\text{m}$ -period fiber grating*, OPT. COMM. 171 (1999): 65-69